Diagonal parameter shifts due to nearest-neighbor displacements in empirical tight-binding theory

Timothy B. Boykin,

Department of Electrical and Computer Engineering, The University of Alabama in Huntsville, Huntsville, Alabama 35899

Gerhard Klimeck, R. Chris Bowen, and Fabiano Oyafuso,

Jet Propulsion Laboratory, California Institute of Technology, 4800 Oak Grove Road, MS 169-315, Pasadena, California 91109

Nano-scale heterostructures are generally characterized by local strain variations. Because the atoms in such systems can be irregularly positioned, theroretical models and parameterizations that are restricted to hydrostatic and uniaxial strain are generally not applicable. To address this shortcoming, a method that enables the incorporation of general distortions into the empirical tight binding model is presented. The method shifts the diagonal Hamiltonian matrix elements due to displacements of neighboring atoms from their ideal bulk positions. The new, efficient, and flexible method is developed for zincblende semiconductors and employed to calculate gaps for GaAs and InAs under hydrostatic and uniaxial strain. Where experimental and theoretical data are available our new method compares favorably with other methods, yet it is not restricted to the cases of uniaxial or hydrstatic strain. Because our method handles arbitrary nearest-neighbor displacements it permits the incorporation of diagonal parameter shifts in general, three-dimensional nano-scale electronic structure simulations, such as the nanoelectronic modeling tool (NEMO 3D).

PACS index: 71.15.-m, 71.23.-k

I. INTRODUCTION

Since the pioneering work of Slater and Koster[1], empirical tight-binding models have provided a convenient and accurate method for modeling semiconductors. Later work by Vogl, Hjalmarson, and Dow[2] and Jancu. et al.[3], has further improved tight-binding models by demonstrating that important gaps and masses can be better fit by models which include an exicted *s*-like orbital, *s** (Ref. 2), and exicted-*d* orbitals (Ref. 3). Tight-binding models have enjoyed considerable success in semiconductor heterostructure calculations in a wide variety of materials systems, some of which involve strain. In such systems highly accurate modeling requires modifying the Hamiltonian matrix elements to take into account the displacements of the atoms from their positions in an unstrained material.

In such strained systems the most obvious modification is to adjust the matrix elements involving orbitals centered on different atoms to take into account the altered environment in terms of both bond angle and length. Bond length alterations are generally included by scaling the Slater-Koster[1] two-center integrals from which the matrix elements are constructed by a factor $\left(d_0/d\right)^{\eta}$, where d_0 (d) is the ideal (altered) bond length.[3-6] This modification is a generalized version of Harrison's[7] d^{-2} scaling law[8]. Changes in the bond angle are automatically incorporated via the direction cosines in the Slater-Koster[1] tables of matrix elements in terms of the two-center integrals.

Since the atomic-like orbitals of tight-binding models are not true atomic orbitals (more typically they are the orthogonalized Löwdin orbitals[9]), it is clear that in principle, the diagonal matrix elements, too, might vary in response to displacements of neighboring atoms. In the case of uniaxial [001] strain, which lifts the degeneracy of the diagonal p_z- and d_{xy}- energies versus their (p_x-, p_y-) and (d_{yz}-, d_{zx}-) counterparts, differing

treatments of the diagonal matrix elements have been suggested. Priester, et al.[4] achieve a good fit for the spin-orbit sp^3s^* model without adjusting the diagonal *p*-matrix elements. Others, however, model the effect of the strain by introducing a new fitting parameter which alters the diagonal *p*- or *d*-matrix elements in proportion to the strain.[3, 6] Tserbak, et al.[6], include a diagonal *p*-matrix element shift in their third-near neighbor sp^3s^* model, while Jancu, et al.[3], shift only the diagonal *d*-matrix elements in their $sp^3d^5s^*$ model. Thus the degree to which such diagonal parameter adjustments are needed appears model dependent.

In those models requiring diagonal parameter shifts, the effect can be dramatic, as illustrated in Fig. 1. Here we plot the conduction- and valence-band edges of GaAs under uniaxial strain using the $sp^3d^5s^*$ model and parameters and scaling exponents of Ref. 3 both with and without their special diagonal *d*-only matrix element adjustment. The differences are striking, especially for the light-hole band edge, which is highly inaccurate when the shifts are turned off. Since diagonal parameter adjustments are required for the $sp^3d^5s^*$ model in the case of uniaxial [001] strain, it expected that they will be necessary for the more general case of irregular displacements of neighboring atoms. Although the modification of Ref. 3 is readily implemented and is entirely satisfactory for systems in which *only* uniaxial strain is present, it is not easily extended to the more general case of strained quantum dots, where displacements are, from the electronic structure perspective, arbitrary, and in which one cannot define a global strain tensor. A more general approach is therefore needed.

Here we present a method for adjusting the diagonal Hamiltonian matrix elements to take into account more general differences in neighboring atoms. Although our method

is in no way restricted to regular distortions of the crystal, such as one encounters under both hydrostatic and uniaxial [001] strain, we use these commonly modeled cases to test the predictions of our approach. In Sec. II we discuss the model and in Sec. III the results, comparing them to **kp**, and experimental results. We present our conclusions in Sec. IV.

II. MODEL

The modifications to the diagonal- and neighboring-atom Hamiltonian matrix elements due to displacements of the atoms in a non-ideal (e.g., strained) crystal take different forms. (In our model we do not alter the spin-orbit matrix elements.) For neighboring-atom matrix elements the changes in bond angle appear through the direction cosines in the Slater-Koster[1] tables. We adjust the magnitudes of the two-center integrals in the Slater-Koster[1] tables using the customary generalization of Harrison's[7] d^{-2} scaling law: $U = U_0\left(d_0/d\right)^{\eta}$, where U_0 is an ideal-crystal two-center integral and d_0 and d are the ideal and actual bond lengths, respectively[8]. Below we discuss adjusting the diagonal Hamiltonian matrix elements.

The starting point for our treatment of diagonal parameter shifts is the Löwdin orthogonalization procedure,[9] which, for a true atomic orbital of type α on the i-th atom, $\left|\Phi_{i,\alpha}\right\rangle$, generates an orthonormal atomic-like orbital of the same type on the same atom, $\left|\varphi_{i,\alpha}\right\rangle$. Because our aim is a treatment suitable for strained quantum dot systems, in which diagonalizing the Hamiltonian is quite costly, it is essential to expend minimum effort on Hamiltonian construction, and a reasonable tradeoff between accuracy and speed is desirable. We therefore drop all overlaps and Hamiltonian matrix elements beyond nearest-neighbor so that the Löwdin procedure[9]gives:

$$\left|\varphi_{i,\alpha}\right\rangle \approx \left|\Phi_{i,\alpha}\right\rangle - \frac{1}{2}\sum_{j,\beta} S_{(j,\beta),(i,\alpha)}\left|\Phi_{j,\beta}\right\rangle \tag{1}$$

$$S_{(j,\beta),(i,\alpha)} = \left\langle \Phi_{j,\beta}\middle|\Phi_{i,\alpha}\right\rangle - \delta_{i,j}\delta_{\alpha,\beta}, \tag{2}$$

where atomic orbitals on the same atom are assumed orthogonal. The diagonal parameters of an empirical tight-binding model are the Löwdin matrix elements $\varepsilon_{i,\alpha} = \left\langle \varphi_{i,\alpha}\middle|\hat{H}\middle|\varphi_{i,\alpha}\right\rangle$, which differ from their free atom counterparts, $\varepsilon_{i,\alpha}^{(0)} = \left\langle \Phi_{i,\alpha}\middle|\hat{H}_i\middle|\Phi_{i,\alpha}\right\rangle$, due to the neighboring-atom contributions in eq. (1). We neglect all other effects such as charge transfer. Given our need for computational efficiency and the approximations we must make for the generally larger (net) overlap effects below, this seems reasonable. (Most tight-binding models in fact omit the effects of charge transfer on the diagonal matrix elements, even for polar semiconductors; see sec. 2.3-E of Ref. 7 for an excellent discussion). Likewise, in the spirit of the bulk model, which ignores same-atom *s*-*s** matrix elements, we exclude any (small) Hamiltonian matrix elements between same-atom orbitals of different symmetry that might arise due to an asymmetric deformation.

We now make three further simplifying restrictions: (i) the atomic orbitals are real; (ii) there are no common nearest-neighbors for a given nearest-neighbor pair; and (iii) only two-center integrals are significant. Restriction (iii) yields the particularly useful approximation for matrix elements between atomic orbitals on different ($n \neq n'$) atoms,

$$v_{(n',\mu'),(n,\mu)}^{(0)} \approx \frac{1}{2}\left[\varepsilon_{n',\mu'}^{(0)} + \varepsilon_{n,\mu}^{(0)}\right] S_{(n',\mu'),(n,\mu)} + \frac{1}{2}\left\langle \Phi_{n',\mu'}\middle|\hat{V}_n + \hat{V}_{n'}\middle|\Phi_{n,\mu}\right\rangle \tag{3}$$

where $\hat{H}_j$ is the free-atom Hamiltonian and $\hat{V}_j$ the potential for the *j*-th atom, $\hat{H}_j\left|\Phi_{j,\nu}\right\rangle = \varepsilon_{j,\nu}^{(0)}\left|\Phi_{j,\nu}\right\rangle$, and $\left\langle \Phi_{n',\mu'}\middle|\hat{H}_n\middle|\Phi_{n,\mu}\right\rangle \approx \varepsilon_{n,\mu}^{(0)} S_{(n',\mu'),(n,\mu)}$. In determining the corresponding Löwdin-orbital matrix element using eq. (1) and assumption (i) above,

observe that under restriction (ii) the only surviving Hamiltonian matrix elements in the sums are those for orbitals centered on the same atom. Consistent with our retention of only the two-center integrals we take $\left\langle \Phi_{i,\alpha} \middle| \hat{H} \middle| \Phi_{i,\beta} \right\rangle \approx \varepsilon_{i,\alpha}^{(0)} \delta_{\alpha,\beta}$ and obtain:

$$v_{(n',\mu'),(n,\mu)} \approx \frac{1}{2} \left\langle \Phi_{n',\mu'} \middle| \hat{V}_n + \hat{V}_{n'} \middle| \Phi_{n,\mu} \right\rangle \tag{4}$$

To proceed any further we must make some approximation concerning the overlap $S_{(n',\mu'),(n,\mu)}$, or equivalently the relationship between $v_{(n',\mu'),(n,\mu)}$ and $v_{(n',\mu'),(n,\mu)}^{(0)}$. Harrison[7] observes that in the extended Hückel theory[10] $S_{i,j} = 2cV_{i,j} \big/ \left(\varepsilon_i + \varepsilon_j \right)$ where *c* is a universal constant; the results of Wills and Harrison[11] show that this is not an unreasonable approximation. We therefore adopt a modified version of this approximation, taking:

$$S_{(n',\mu'),(n,\mu)} = K_{(n',\mu'),(n,\mu)} \frac{v_{(n',\mu'),(n,\mu)}}{\varepsilon_{n',\mu'}^{(0)} + \varepsilon_{n,\mu}^{(0)}}, \quad n \neq n' \tag{5}$$

or, equivalently, substituting eq. (4) into eq. (3),

$$v_{(n',\mu'),(n,\mu)}^{(0)} \approx \frac{2 + K_{(n',\mu'),(n,\mu)}}{2} v_{(n',\mu'),(n,\mu)} \tag{6}$$

where the constants $K_{(n',\mu'),(n,\mu)}$ depend upon the orbitals involved in the matrix element, in order to provide greater flexibility in fitting the properties of strained materials. The constants *K* are of course symmetric, $K_{(n',\mu'),(n,\mu)} = K_{(n,\mu),(n',\mu')}$, and the subscripts n and n' on $K_{(n',\mu'),(n,\mu)}$ imply only a dependence on atomic species, *not* on position. The orbital types μ, μ' in eqs. (5) and (6) are the customary atomic-like orbitals (*sa*, *sc*, $p_x a$, $d_{xy} c$, etc.), with the matrix elements $v_{(n',\mu'),(n,\mu)}$ calculated from the Slater-Koster tables.[1] In an attempt to limit the number of additional parameters we restrict the *K* to depend only upon species and total angular momentum ($K_{sa,pc}$, $K_{d,d}$, etc.), ignoring any dependence on

bond type ($dd\pi, pp\sigma$, etc.). The atomic energies $\varepsilon_{j,\nu}^{(0)}$ are vacuum-referenced and hence the overlaps will have the proper sign for $K > 0$.

Using eqs. (5) and (6) in (3) we find that the diagonal Hamiltonian matrix elements are related to their free-atom counterparts via

$$\varepsilon_{i,\alpha} \approx \varepsilon_{i,\alpha}^{(0)} - \sum_{\substack{j,\beta \\ j \in NN-i}} C_{(j,\beta),(i,\alpha)} \frac{v_{(j,\beta),(i,\alpha)}^2}{\varepsilon_{j,\beta}^{(0)} + \varepsilon_{i,\alpha}^{(0)}} \tag{7}$$

$$C_{(j,\beta),(i,\alpha)} = \frac{1}{2}\left[2K_{(j,\beta),(i,\alpha)} + K_{(j,\beta),(i,\alpha)}^2\right] \tag{8}$$

Eq. (7) leads directly to our real objective, a relationship between the diagonal tight-binding matrix elements in the ideal (unprimed) and altered (primed) nominally-zincblende systems:

$$\varepsilon'_{i,\alpha} = \varepsilon_{i,\alpha} + \sum_{\substack{j,\beta \\ j \in NN-i}} C_{(j,\beta),(i,\alpha)} \frac{v_{(j,\beta),(i,\alpha)}^2 - v'^2_{(j,\beta),(i,\alpha)}}{\varepsilon_{j,\beta} + \varepsilon_{i,\alpha}} \tag{9}$$

where in eq. (9) we have replaced the atomic energies $\varepsilon_{n,\mu}^{(0)}$ by their ideal, vacuum-referenced Löwdin orbital counterparts (i.e., we apply an identical downward shift to all diagonal bulk tight-binding parameters so that they are negative). Note that the resulting difference in $\varepsilon'_{i,\alpha}$ will be roughly of magnitude $\left[v_{i,j}/\left(\varepsilon_i + \varepsilon_j\right)\right]^2$.

In spite of the simplifications made in order to obtain a computationally efficient formula, we see that eq. (9) has the highly desirable property that it automatically incorporates changes in geometry due to displacements of the atoms since the $v_{(j,\beta),(i,\alpha)}$ and $v'_{(j,\beta),(i,\alpha)}$ involve direction cosines for the ideal and altered crystals, respectively. Hence arbitrary displacements of neighboring atoms are implicitly included in the diagonal parameter shift and there is no need to separately model cases of hydrostatic or

uniaxial strain, for example. Note as well that the diagonal parameter shifts are no longer linear in the strain, since the $v_{(j,\beta),(i,\alpha)}$ and $v'_{(j,\beta),(i,\alpha)}$ are not necessarily linear and they furthermore appear squared.

III. RESULTS

In Table I we list the two-center integrals in our parameterization for GaAs and InAs in the Slater-Koster[1] notation for the $sp^3d^5s^*$ model.[3] As a convenience we choose the same diagonal parameter for all *d*-orbitals of a given species in bulk, although in principle we could have chosen different energies for $\left(d_{xy}, d_{yz}, d_{zx}\right)$ and $\left(d_{3z^2-r^2}, d_{x^2-y^2}\right)$ due to the crystal-field splitting. The lowest twenty (20) bulk bands of GaAs and InAs are shown in Figures 2 and 3, respectively. In Table II we list the energies and effective masses reproduced by the parameters of Table I. These parameters are determined using our genetic algorithm[12] and it is evident that they provide a good fit to technologically important energies and masses of both bulk materials. Note that our parameterizations are chosen to reproduce the room-temperature gaps and that the valence-band maximum of GaAs is chosen as the reference energy. The InAs valence-band maximum is offset relative to that of GaAs since the parameters are ultimately employed in modeling InAs/GaAs heterostructures such as quantum dots[13].

In Table III we list the parameters for strained systems, which were fit to reproduce the conduction-band, and light-, heavy-, and split-off-hole valence-band edges at Γ under hydrostatic pressure and uniaxial strain. Because the split-off hole is not of great interest to us in quantum dot modeling, we assigned it only small weights in the fitting procedure. As mentioned above the two-center integrals are scaled with the generalized version of

Harrison's[7] d^{-2} scaling law, $U = U_0\left(d_0/d\right)^{\eta}$, where U_0 is a bulk two-center integral, U its counterpart in the strained material, η the exponent, and d_0 and d are the ideal (bulk) and actual (strained) bond length, respectively. The constants, C, are listed as well; the overlap constants K are given by the positive root of eq. (8). Since the cases of hydrostatic pressure and uniaxial strain have been treated theoretically,[14] and for GaAs under hydrostatic pressure, experimentally[15], we next discuss the behavior of our model under these conditions.

We first consider the positions of the valence and conduction-band edges at Γ under hydrostatic deformation, $\varepsilon_{xx} = \varepsilon_{yy} = \varepsilon_{zz} = \varepsilon$. Negative ε corresponds to a conventional hydrostatic pressure experiment, positive ε to a uniform dialation, which is of interest for quantum dots in which such atomic displacements can occur. We plot these for GaAs and InAs as calculated with our model and **kp** theory[14] in fig. 4; the results for InAs are similar. The parameters appearing in the **kp** formulas are taken from Van de Walle.[14] For both GaAs and InAs (not shown) the trends are similar in both approaches. In fig. 5 we plot the direct and indirect gaps of GaAs under hydrostatic pressure as calculated with our model versus the measurements of Goñi, et al.[15] In our model both gaps are somewhat less pressure-sensitive than the measured values, and in our parameterization the direct-indirect crossover occurs at $|\varepsilon| \approx 0.02$ whereas the experimental value is about 0.016. The agreement with the indirect gap result is especially encouraging with regards to the physical content of the model, since the model was *not* explicitly parameterized to fit indirect-gap data. In view of the significant experimental uncertainties and the generality of our approach, which is not limited to only hydrostatic pressure or uniaxial strain, the agreement is good. Finally we mention that although at zero pressure all *d*-

orbitals of the same species have the same energy, under hydrostatic pressure the crystal-field splitting appears in our model. It is largest for GaAs, about 0.165 eV at $|\varepsilon| = 0.05$, but even so is still less than 2% of the zero-pressure *d*-energy.

We next study the case of uniaxial [001] strain. Here to facilitate comparison with the **kp** results we calculate ε_{zz} as a function of $\varepsilon_{xx} = \varepsilon_{yy} = \varepsilon_{\|}$ using Van de Walle's[14] values for D^{001}. In fig. 6, we plot the shifts for GaAs of E_z and E_{xy} relative to their zero-strain values as functions of $\varepsilon_{\|}$. Note that the vast majority of the change is reflected in the *p*-orbitals (E_z) – the *d*-orbitals (E_{xy}) are relatively unaffected. In fig. 7 we plot the band edges of GaAs versus $\varepsilon_{\|}$ for both our model and the **kp** model, with parameters from Van de Walle.[14] Both models display the same trends, with the exception of the split-off hole band. (Note, however, that GaAs, has a relatively small lattice constant and will generally be stretched, not compressed, in InGaAs/GaAs quantum dot simulations[13].) Finally we mention that the nonlinear strain behavior of the tight-binding conduction-band edge (fig. 7) appears to be at least partly related to the total *s**-contribution to the zero-strain state. In a tight-binding model with *s*-*s** coupling, each of the two degenerate zero-strain conduction-band states at Γ belongs to a four-dimensional subspace $\{|sa\rangle, |sc\rangle, |s*a\rangle, |s*c\rangle\}$, and those states with larger total *s**-contribution tend to be more nonlinear in the strain.

IV. CONCLUSIONS

Because the $sp^3d^5s^*$ model requires diagonal parameter shifts to correctly model uniaxial [001] strain, we have developed a general treatment which adjusts diagonal tight-binding parameters for zincblende crystals due to arbitrary nearest-neighbor

displacements. Our method is in no way restricted to regular distortions. We have shown that this method correctly reproduces the altered geometry of the rearranged atoms. In order to test the method we have compared its results for hydrostatic pressure and uniaxial [001] strain to those of **kp** and other tight-binding approaches. We find that this method provides good agreement with other calculations and, unlike special diagonal shift formulas for uniaxial strain only, treats arbitrary cases naturally and automatically. Our method is efficient to implement for nearest-neighbor models, making it well-suited to use for modeling quantum heterostructures where a minimum of effort can be expended on Hamiltonian construction in multimillion atom quantum dot simulations[13].

ACKNOWLEDGEMENTS

TBB thanks Prof. Walter A. Harrison for several valuable discussions. Part of this work was carried out at Jet Propulsion Laboratory under a contract with the National Aeronautics and Space Administration (NASA). The supercomputer used in this investigation was provided by funding from the NASA Offices of Earth Science, Aeronautics, and Space Science. This work, at both the Jet Propulsion Laboratory and the University of Alabama in Huntsville, was supported in part by the Advanced Research and Development Activity (ARDA) under contract number XXXXXXXXX.

REFERENCES

[1]J. C. Slater and G. F. Koster, Phys. Rev. **94**, 1498 (1954).

[2]P. Vogl, Harold P. Hjalmarson, and John D. Dow, J. Phys. Chem. Solids **44**, 365 (1983).

[3]Jean-Marc Jancu, Reinhold Scholz, Fabio Beltram, and Franco Bassani, Phys. Rev. B **57**, 6493 (1998).

[4]C.Priester, G. Allan, and M. Lannoo, Phys. Rev. B **37**, 8519 (1988).

[5]L. Brey, C. Tejedor, and J. A. Vergés, Phys. Rev. B **29**, 6840 (1984).

[6]C.Tserbak, H. M. Polatoglou, and G. Theodorou, Phys. Rev. B **47**, 7104 (1993).

[7]Walter A. Harrison, *Elementary Electronic Structure* (World Scientific, New Jersey, 1999).

[8]Typical values for the exponent η are in the range 1-4.

[9]Per-Olov Löwdin, J. Chem. Phys. **18**, 365 (1950).

[10]R. Hoffman, J. Chem. Phys. **39**, 1397 (1963).

[11]John M. Wills and Walter A. Harrison, Phys. Rev. B **28**, 4363 (1983).

[12]Gerhard Klimeck, R. Chris Bowen, Timothy B. Boykin, Carlos Salazar-Lazaro, Thomas A. Cwik, and Adrian Stoica, Sup. Microst. **27**, 77 (2000); Gerhard Klimeck, R. Chris Bowen, Timothy B. Boykin, and Thomas A. Cwik, Sup. Microst. **27**, 519 (2000).

[13]Gerhard Klimeck, Fabiano Oyafuso, Timothy B. Boykin. R. Chris Bowen, and Paul von Allmen, J. Comp. Mod. Eng. Sci. (invited, in press).

[14]Chris G. Van de Walle, Phys. Rev. B **39**, 1871 (1989); F. H. Pollack and M. Cardona, Phys. Rev, **172**, 816 (1968). Because Van de Walle gives low-temperature parameters, we have reduced the **kp** conduction-band energy (to equalize zero pressure gaps) and then uniformly shifted all **kp** band edges to align them with our edges at zero pressure.

[15]A. R. Goñi, K. Strössner, K. Syasser, and M. Cardona, Phys. Rev. B **36**, 1581 (1987).

[16]Available experimental data are taken from *Semiconductors: Group IV Elements and III-V Compounds*, ed. O. Madelung (Springer, New York, 1991). Note in particular that room-temperature values of the indirect gaps are generally not well-known. We therefore assume that the room-temperature Γ-*L* and Γ -*X* separations are the same as the low-temperature values. In addition, many effective masses, especially those of the *X*- and *L*-valleys, are not definitively known for InAs. Here we have chosen target values typical of other III-V materials. Finally, the InAs-GaAs valence-band offset built into our

parameters has not been precisely determined. Our target value has given good results in multiband transport simulations of resonant tunneling diodes and other one-dimensional quantum-confinement structures.

TABLES

Table I: Lattice constants, diagonal and spin-orbit parameters, and two-center integrals for our parameterizations of GaAs and InAs in the $sp^3d^5s^*$ model. E_{shift} is the downward atomic shift applied to the diagonal parameters prior to determining alterations due to displacements of nearest-neighbors. The same upward shift is then applied to the altered diagonal parameters. Lattice constants are in Å; all other values are in eV.

Parameter	GaAs	InAs
a	5.6532	6.0583
E_{sa}	-5.500420	-5.500420
E_{pa}	4.151070	4.151070
E_{sc}	-0.241190	-0.581930
E_{pc}	6.707760	6.971630
E_{s^*a}	19.710590	19.710590
E_{s^*c}	22.663520	19.941380
E_{da}	13.031690	13.031690
E_{dc}	12.748460	13.307090
E_{shift}	27.000000	27.000000
$ss\sigma$	-1.645080	-1.694350
$s^*s^*\sigma$	-3.704550	-4.210450
$s_a^*s_c\sigma$	-2.207770	-2.426740

$s_a s_c * \sigma$	-1.314910	-1.159870
$s_a p_c \sigma$	2.664930	2.598230
$s_c p_a \sigma$	2.960320	2.809360
$s_a * p_c \sigma$	1.976500	2.067660
$s_c * p_a \sigma$	1.027550	0.937340
$s_a d_c \sigma$	-2.609400	-2.268370
$s_c d_a \sigma$	-2.320590	-2.293090
$s_a * d_c \sigma$	-0.628200	-0.899370
$s_c * d_a \sigma$	-0.133240	-0.488990
$pp\sigma$	4.150800	4.310640
$pp\pi$	-1.427440	-1.288950
$p_a d_c \sigma$	-1.874280	-1.731410
$p_c d_a \sigma$	-1.889640	-1.978420
$p_a d_c \pi$	2.529260	2.188860
$p_c d_a \pi$	2.549130	2.456020
$dd\sigma$	-1.269960	-1.584610
$dd\pi$	2.505360	2.717930
$dd\delta$	-0.851740	-0.505090

λ_a	0.172340	0.172340
λ_c	0.021790	0.131200

Table II: Selected energies (in eV), *k*-minima (in units of π/a) and effective masses (in units of the free-electron mass) for GaAs and InAs as reproduced by the parameters of Table I, along with target values given our fitting algorithm (Ref. 12); see Ref. 16. In both materials the *L*-valley minimum occurs at the symmetry point. All masses are computed at the respective extrema.

Quantity	GaAs	GaAs-Target	InAs	InAs-Target
E_c^{Γ}	1.41280	1.42400	0.59421	0.59570
E_v^{Γ}	-0.00306	0.00000	0.22430	0.22570
Δ_0	0.32647	0.34000	0.39316	0.38000
$E_{c,\min}^{L}$	1.69811	1.70800	1.75315	1.75570
$E_{c,\min}^{X}$	1.89846	1.90000	2.50732	2.50570
$k_{\min}^{[001]}$	1.81358	1.80000	2.00000	1.80000
Electrons				
m_{Γ}	0.06574	0.06700	0.02353	0.02390
$m_{X,l}$	1.88076	1.30000	1.12583	1.30000
$m_{X,t}$	0.17525	0.23000	0.17514	0.23000
$m_{L,l}$	1.72750	1.90000	1.53946	1.90000
$m_{L,t}$	0.09671	0.07540	0.09414	0.07540
Holes				

$m_{lh}^{[100]}$	0.08249	0.08710	0.02811	0.02730
$m_{lh}^{[110]}$	0.07546	0.08040	0.02729	0.02640
$m_{lh}^{[111]}$	0.07362	0.07860	0.02703	0.02610
$m_{hh}^{[100]}$	0.37686	0.40300	0.35158	0.34480
$m_{hh}^{[110]}$	0.65660	0.66000	0.56349	0.63910
$m_{hh}^{[111]}$	0.83905	0.81300	0.69813	0.87640
m_{so}	0.16243	0.15000	0.09959	0.15000

Table III: Dimensionless scaling exponents, η, and diagonal parameter shift constants, *C*, defined in Eq. (8) for GaAs and InAs.

Parameter	GaAs	InAs
$\eta_{s,s\sigma}$	2.060010	1.924940
$\eta_{s,s^*\sigma}$	0.000000	0.060800
$\eta_{s^*,s^*\sigma}$	0.212660	0.000810
$\eta_{s,p\sigma}$	1.384980	1.570030
$\eta_{s^*,p\sigma}$	1.399300	1.949370
$\eta_{s,d\sigma}$	1.898890	1.765660
$\eta_{s^*,d\sigma}$	1.785400	2.023870
$\eta_{p,p\sigma}$	2.684970	2.061510
$\eta_{p,p\pi}$	1.314050	1.602470
$\eta_{p,d\sigma}$	1.812350	2.383820
$\eta_{p,d\pi}$	2.379640	2.455600
$\eta_{d,d\sigma}$	1.724430	2.322910
$\eta_{d,d\pi}$	1.972530	1.615890
$\eta_{d,d\delta}$	1.896720	2.329600
$C_{s,s}$	0.586960	1.258286
C_{s^*,s^*}	0.486090	2.481447
C_{sa,s^*c}	0.770950	4.557774

$C_{s*a,sc}$	0.889210	1.086223
$C_{sa,pc}$	0.759790	4.367575
$C_{sc,pa}$	1.458910	7.029660
$C_{s*a,pc}$	0.810790	3.298598
$C_{s*c,pa}$	1.212020	7.029496
$C_{sa,dc}$	1.070150	0.000000
$C_{sc,da}$	0.580530	0.187036
$C_{s*a,dc}$	1.032560	1.195042
$C_{s*c,da}$	1.323850	1.769483
$C_{p,p}$	2.000000	4.624438
$C_{pa,dc}$	1.613500	0.000000
$C_{pc,da}$	1.500000	0.000000
$C_{d,d}$	1.262620	0.246999

FIGURE CAPTIONS

Figure 1: Conduction- and valence-band edges of GaAs in the parameterization of Ref. 3 as calculated with and without their special diagonal *d*-matrix element shift.

Figure 2: The lowest 20 bands of GaAs as reproduced by the parameters of Table I.

Figure 3: The lowest 20 bands of InAs as reproduced by the parameters of Table I.

Figure 4: GaAs band edges under hydrostatic deformation as calculated with our model and the **kp** model of Van de Walle (Ref. 14, adjusted to reflect room-temperature gaps). Negative ε corresponds to conventional hydrostatic pressure experiments, positive ε to a uniform dialation.

Figure 5: Direct and indirect band gaps of GaAs band edges under hydrostatic pressure as calculated with our model and as measured (Ref. 15).

Figure 6: Diagonal *p*- $\left[\Delta E\left(p_z \mu\right)\right]$ and *d*- $\left[\Delta E\left(d_{xy} \mu\right)\right]$ parameter shifts relative to their respective zero-strain values $\left(E_{p\mu}, E_{d\mu}\right)$ for GaAs under uniaxial strain as calculated with our model.

Figure 7: GaAs band edges under uniaxial strain as calculated with our model and the **kp** model of ref. 14, adjusted to reflect room-temperature gaps.

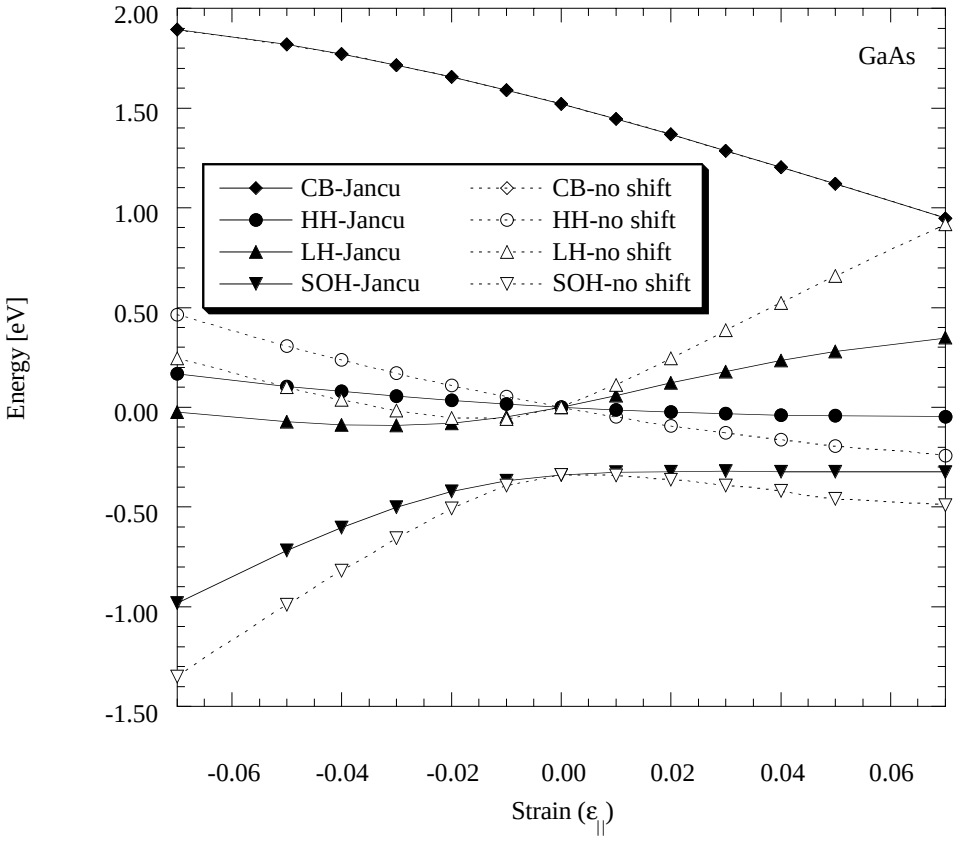
GaAs
CB-Jancu
HH-Jancu
LH-Jancu
SOH-Jancu
CB-no shift
HH-no shift
LH-no shift
SOH-no shift
Energy [eV]
2.00
1.50
1.00
0.50
0.00
-0.50
-1.00
-1.50
-0.06
-0.04
-0.02
0.00
0.02
0.04
0.06
Strain (ε||)

Figure 1

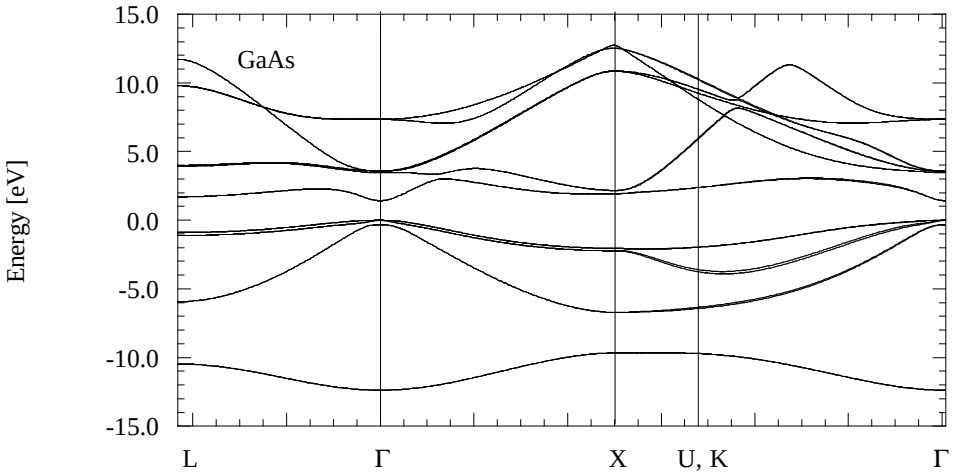

Figure 2

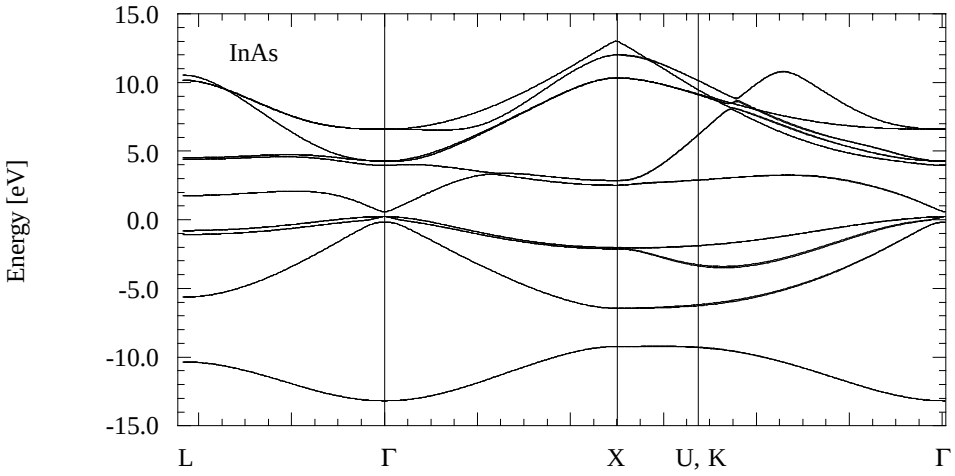

Figure 3

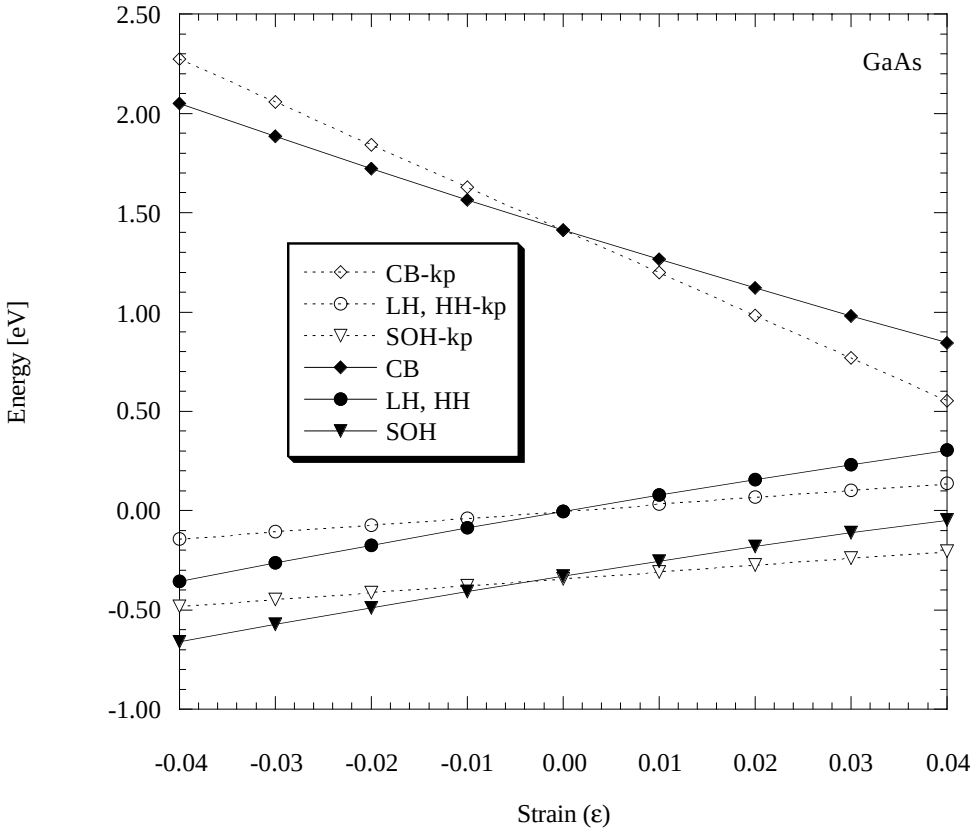
GaAs
CB-kp
LH, HH-kp
SOH-kp
CB
LH, HH
SOH
Energy [eV]
Strain (ε)
2.50
2.00
1.50
1.00
0.50
0.00
-0.50
-1.00
-0.04
-0.03
-0.02
-0.01
0.00
0.01
0.02
0.03
0.04

Figure 4

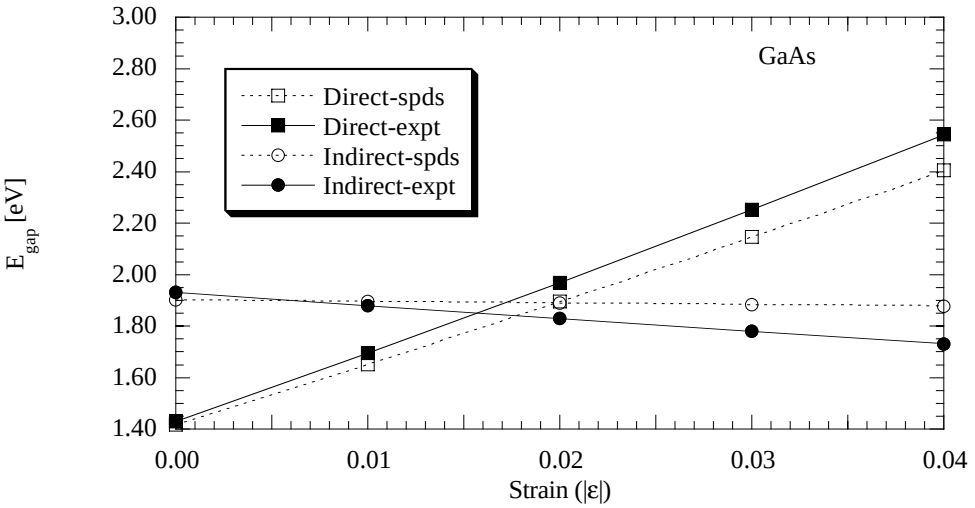
GaAs
Direct-spds
Direct-expt
Indirect-spds
Indirect-expt
E gap [eV]
3.00
2.80
2.60
2.40
2.20
2.00
1.80
1.60
1.40
0.00
0.01
0.02
0.03
0.04
Strain (|ε|)

Figure 5

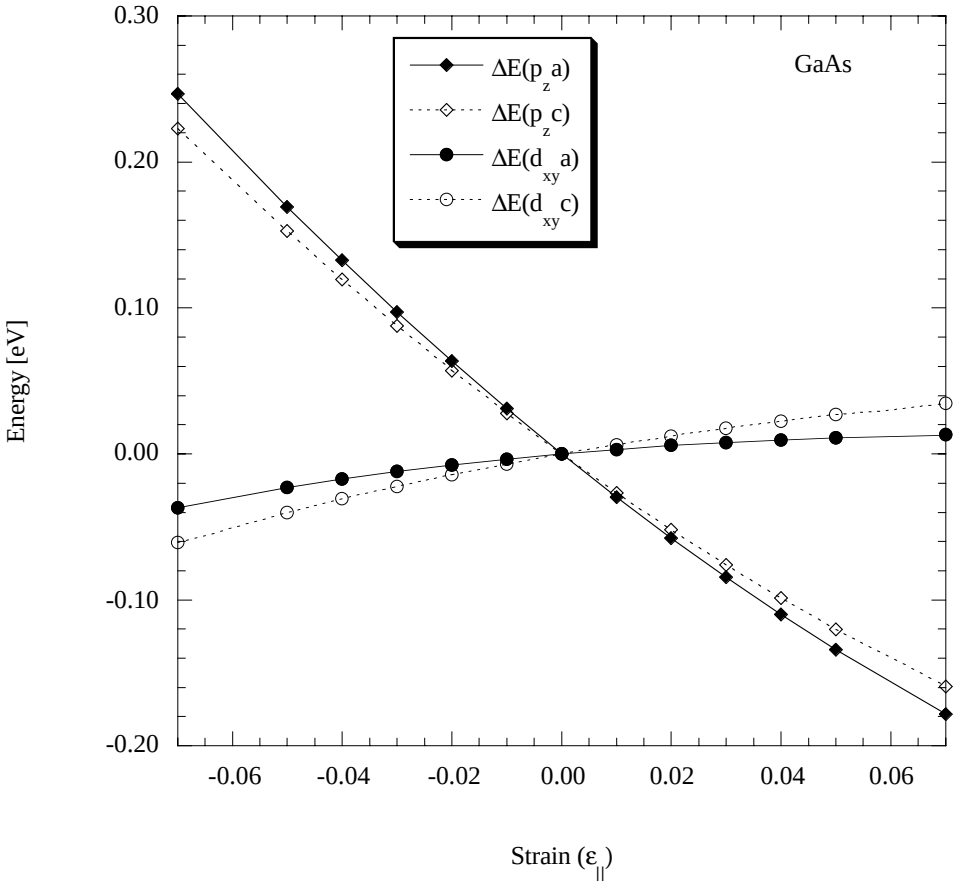
GaAs
ΔE(p_z a)
ΔE(p_z c)
ΔE(d_xy a)
ΔE(d_xy c)
Energy [eV]
0.30
0.20
0.10
0.00
-0.10
-0.20
-0.06
-0.04
-0.02
0.00
0.02
0.04
0.06
Strain (ε_||)

Figure 6

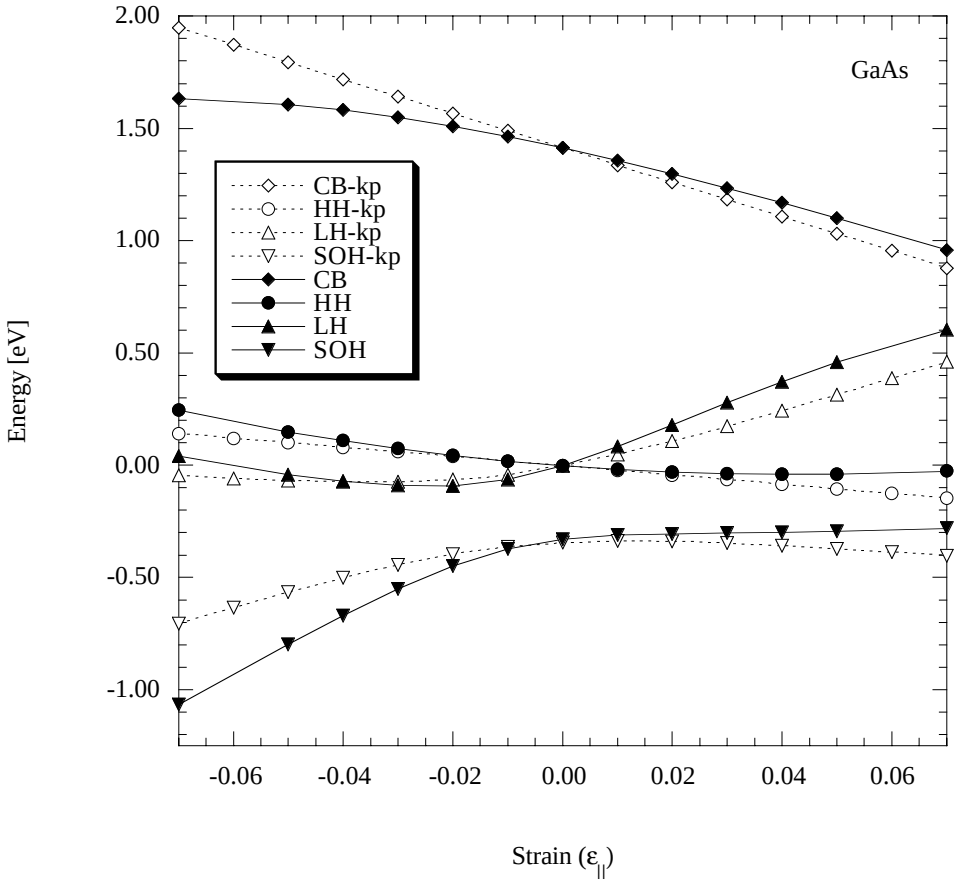
GaAs
CB-kp
HH-kp
LH-kp
SOH-kp
CB
HH
LH
SOH
2.00
1.50
1.00
0.50
0.00
-0.50
-1.00
-0.06
-0.04
-0.02
0.00
0.02
0.04
0.06
Energy [eV]
Strain (ε||)

Figure 7